FINAL REMARKS

The procedure for the evaluation of the attractive term in a van der Waals type of equation allows introduction in the equation of state of the exact values of the vapor pressure of pure components.

This makes the equation of state applicable to all compounds and to the whole temperature range, and more accurate in the prediction of both multicomponent and pure vapor-liquid equilibria. This procedure gives a qualitative description of the effects of the presence of nonvolatile components on the multicomponent vapor-liquid equilibria, using only informations about the influence of the electrolyte on pure components.

Of course, the quantitative agreement with the experimental data can be improved by giving a description of the influence of the electrolytes on pure compounds, which is more accurate than Eq. 20. Besides, the introduction of a semi-empirical interaction parameter in the mixing rule (Eq. 19) will contribute to a better quantitative description of the system under examination, either with or without nonvolatile components.

ACKNOWLEDGMENTS

Thanks are due to Consiglio Nazionale delle Ricerche for financial aid. The authors are grateful to F. Lotito and L. Toppo for their valuable help with the computations.

NOTATION

b = parameter of the equation of state
f_i = fugacity of component i
P = pressure
p_i^0 = vapor pressure of component i
T = temperature
V = volume
V^* = covolume
x_i = mole fraction of component i in the liquid phase
y_i = mole fraction of component i in the vapor phase
Z = compressibility factor
Z^{hs} = hard sphere compressibility factor
φ = fugacity coefficient

Superscripts

l = liquid phase
v = vapor phase
s = nonvolatile compound

Subscripts

C = value at the critical point
R = reduced value

LITERATURE CITED

Anderson, T. F. and J. M. Prausnitz, "Computational Methods for High Pressure Phase Equilibria and Other Fluid-Phase Properties Using a Partition Function: 2. Mixtures," *Ind. Eng. Chem. Proc. Des. and Dev.*, **19**, 9 (1980).

Beret, S. and J. M. Prausnitz, "Perturbed Hard-Chain Theory: An Equation of State for Fluids Containing Small or Large Molecules," *AIChE J.*, **21**, 1123 (1975).

Carnahan, N. F. and K. E. Starling, "Intermolecular Repulsions and the Equation of State for Fluids," *AIChE J.*, **18**, 1184 (1972).

Cruccu, M., S. Dernini, and R. De Santis, "Effetti Sale Nell'Equilibrio Liquido-Vapore di Sistemi Binari," *Chim. Ind.*, **57**, 459 (1975).

Dernini, S., R. De Santis, and F. Gironi, "Un Metodo di Correlazione di Equilibri Liquido-Vapore in Presenza di Elettroliti Non Volatili," *An. di Chim.*, **65**, 409 (1975).

Dernini, S., R. De Santis, and L. Marrelli, "Salt Effects on Isobaric Vapor-Liquid Equilibria of Acetone-Methanol System," *J. Chem. Eng. Data*, **21**, 170 (1976).

Gmehling, J., D. D. Liu, and J. M. Prausnitz, "High-Pressure Vapor-Liquid Equilibria for Mixtures Containing One or More Polar Components," **34**, 951 (1979).

Hirata, M., S. Ohe, and K. Nagahama, *Computer-Aided Data Book of Vapor-Liquid Equilibria*, Elsevier Scientific Publishing Company, New York (1975).

Murti, P. S. and M. van Winkle, "Vapor-Liquid Equilibria for Binary Systems of Methanol, Ethyl Alcohol, 1-Propanol and 2-Propanol with Ethyl Acetate and 1-Propanol-Water," *J. Chem. Eng. Data. Series*, **3**, 72 (1958).

Ohe, S., K. Yokoyama, and S. Nakamura, "Salt Effect in Vapor-Liquid Equilibria of Methanol, Ethyl Acetate-Calcium Chloride System," *J. Chem. Eng. Data*, **16**, 70 (1971).

Peng, D. Y. and D. B. Robinson, "A New Two-Constant Equation of State," *Ind. Eng. Chem. Fund.*, **15**, 59 (1976).

Ross, A. and W. R. Supina, "Vapor Pressure and Vapor-Liquid Equilibrium Data for Methyl Esters of the Common Saturated Normal Fatty Acids," *J. Chem. Eng. Data*, **6**, 173 (1961).

Soave, G., "Equilibrium Constants from a Modified Redlich-Kwong Equation of State," *Chem. Eng. Sci.*, **27**, 1197 (1972).

Wichterle, I., "High-Pressure Vapor-Liquid Equilibrium: IV," *Fluid Phase Equilibria*, **2**, 59 (1978).

Manuscript received April 28, 1980; revision received October 7, and accepted October 20, 1980.

Diffusion and Reaction in a Stagnant Boundary Layer About a Carbon Particle

Part 7: Transient Behavior and Effect of Water Vapor

S. SUNDARESAN
and
NEAL R. AMUNDSON
University of Houston, Houston, TX 77004

The dynamics of carbon combustion is studied. It is shown that the carbon particle will not ignite if the furnace temperature is below a certain critical value. In addition, carbon particles display thermal instabilities which can be delayed or eliminated by increasing the water vapor concentration and/or the furnace temperature.

SCOPE

Due to its practical importance the combustion of carbon has attracted an enormous amount of theoretical and experimental work. Carbon combustion involves an interaction of heterogeneous and homogeneous reactions, and transport limitations. This gives rise to a complex pathology, understanding which is of fundamental importance in the context of coke

0001-1541-81-4312-0679-$2.00.

fired boilers, char combustors and correct interpretation of the kinetic data. The pseudo steady state structure associated with carbon combustion has previously been identified by employing a model with minimal assumptions. In the present study the dynamics of single particle carbon combustion is analysed and effects of various process variables (e.g., furnace temperature, water vapor concentration, etc.) on carbon combustion are elucidated.

CONCLUSIONS AND SIGNIFICANCE

The dynamics of a single particle carbon combustion, when the O_2 level in the gas phase is large, is studied. When a carbon particle, preheated to a high temperature in an inert atmosphere is introduced into a furnace containing oxygen and a trace of water vapor, the particle burns rapidly at first. It is shown that such an artificially ignited particle will not sustain ignition if the furnace temperature is below some critical value. When a carbon particle, which is initially at a temperature lower than the furnace temperature, is admitted into the furnace, it ignites only above a certain critical furnace temperature.

The water vapor in the gas phase catalyzes the CO oxidation in the boundary layer and the combustion of large carbon particles is always accompanied by significant CO oxidation in the boundary layer. It has been shown that as the particle shrinks during combustion, even if the heterogeneous combustion reactions sustain ignition, the homogeneous CO oxidation is destabilized when the particle size reaches some critical value. This critical particle size decreases if the water vapor level in the gas phase and/or the furnace temperature is increased. The thermal instability observed by Ubhayakar and Williams (1976) during the combustion of small particles is predicted by the model and is shown to be an inevitable feature.

The physical system considered in this paper is a carbon particle surrounded by a stagnant boundary layer through which O_2 diffuses from the ambient gas and reacts with the carbon surface to produce CO. The CO so obtained is oxidized homogeneously to CO_2 in the boundary layer and the resulting CO_2 diffuses in part to the carbon surface where it is reduced to CO. The intraparticle diffusional resistances are lumped at the particle surface and the particle is assumed to burn in a shrinking core fashion. The pseudosteady state behavior of this system was analysed by Amundson and coworkers. The genesis of the complex steady state structure associated with carbon combustion was identified by Sundaresan and Amundson (1980a); and it was shown that the qualitative features of the steady state structure are sensitive to the environment with which the particle is in radiant interaction and the level of O_2 in the ambient gas phase determines the complexity of the steady state structure.

Smith and Gudmundsen (1931) have studied experimentally the combustion of carbon particles in dry as well as humid air. They found that the carbon particles burning in humid air are usually hotter than those burning in dry air (by as much as 70°C) and this temperature difference vanishes as the particle size becomes small. Surprisingly, in spite of the fact that the particles burning in humid air are hotter than (or as hot as) those burning in dry air, the particles were burning at a slower rate in humid air compared to dry air. Water vapor in the gas phase participates in carbon combustion through its catalytic effect on CO oxidation and the reaction between carbon and water vapor. It was shown by Sundaresan and Amundson (1980b) that in order to determine the qualitative features of the steady state structure associated with carbon combustion correctly, it is necessary to include the catalytic effect of water vapor on CO oxidation and that neglecting the reaction between carbon and water vapor does not alter the structure.

Mon and Amundson (1980) have presented some preliminary results on the dynamics of single particle carbon combustion. In this paper, we shall present an analysis of the dynamics on the basis of the steady state structure brought out in our earlier work (1980a) and also examine the effect of water vapor on the dynamics. This work necessarily draws to a great extent on the results of the previously mentioned papers (Caram and Amundson, 1977; Mon and Amundson, 1978, 1980; Sundaresan and Amundson, 1980a, b), which should be consulted before proceeding with this one.

THE MODEL

We consider a spherical carbon particle of radius a, surrounded by a stagnant boundary layer extending to radius b, outside which we have the uniform ambient gas phase. The chemical species present are O_2, CO_2, CO, H_2O and N_2 (inert), and will be denoted by subscripts 1 to 5, respectively. It is assumed that the only effect of water vapor is to catalyse the reaction between CO and O_2. The heterogeneous reactions at the carbon surface are (1) $2C + O_2 = 2CO$, exothermic, $\mathcal{R}_1$(kg ·

TABLE 1. VALUES OF k_i AND E_i.

$\gamma_1 = \gamma_3 = 1.274$

$\gamma_2 = 1.0$

$CD = 1.56 \times 10^{-6}$ kg · mol/m · s

$(-\Delta H_1) = 53725$ kcal/kg · mol

$(-\Delta H_2) = -40690$ kcal/kg · mol

$(-\Delta H_3) = 67550$ kcal/kg · mol

$C_g = 9.36$ kcal/kg · mol · °K

$C_s = 4.17$ kcal/kg · mol · °K

$\rho_s = 1650$ kg/m^3

$\sigma = 1.356 \times 10^{-11}$ $\frac{\text{kcal}}{\text{m}^2 \cdot \text{s} \cdot K^4}$

$\epsilon = 0.93$

$k_1 = 3630$ $\frac{\text{kg} \cdot \text{mol}}{\text{m}^2 \cdot \text{atm} \cdot \text{s}}$

$k_2 = 4.016 \times 10^8$ m/s

$k_3 = 1.3 \times 10^{11}$ $\frac{\text{m}}{\text{s}} \cdot \frac{\text{m}^3}{\text{kg} \cdot \text{mol}}$

$E_1 = 35700$ kcal/kg · mol

$E_2 = 59192$ kcal/kg · mol

$E_3 = 30000$ kcal/kg · mol

$\lambda = 1.3 \times 10^{-5}$ kcal/m · s · °K

mol of $O_2/m^2 \cdot s$); (2) $C + CO_2 = 2CO$, endothermic, $\mathcal{R}_2$(kg · mol of $CO_2/m^2 \cdot s$). In the boundary layer we have the homogeneous reaction (3) $CO + \frac{1}{2}O_2 = CO_2$, exothermic, $\mathcal{R}_3$(kg · mol of $CO/m^3 \cdot s$). We shall employ the kinetic rate expressions proposed by Field et al. (1967), Dutta et al. (1975) and Howard et al. (1973).

$$\mathcal{R}_1 = k_1 \exp(-E_1/RT_s)Py_{1s}$$

$$\mathcal{R}_2 = k_2 \exp(-E_2/RT_s)C_{2s}$$

$$\mathcal{R}_3 = k_3 \exp(-E_3/RT)C_3C_1^{\frac{1}{2}}C_4^{\frac{1}{2}}$$

The values of k_i's and E_i's are listed in Table 1. In a multicomponent system, the fluxes are related to the composition gradient by the Stefan-Maxwell equations:

$$\frac{dy_i}{dr} = \sum_{j=1}^{5} \frac{1}{CD_{ij}} (y_iN_j - y_jN_i), \; i = 1 \text{ to } 5$$

By assuming that the Stefan flow is negligible and the mole fractions of the reactant gases are small, the Stefan-Maxwell equations can be reduced to (Mon and Amundson, 1978):

$$N_i = -\gamma_i CD \frac{dy_i}{dr}, \; i = 1 \text{ to } 3 \tag{1}$$

The flux of sensible heat e, is given by:

$$e = -\lambda \frac{dT}{dr} \tag{2}$$

The conservation equations for mass and energy in the boundary layer have the form:

$$\frac{\partial C_i}{\partial t} = -\frac{1}{r^2}\frac{\partial}{\partial r}(r^2N_i) + \nu_i\mathcal{R}_3, \; i = 1 \text{ to } 3 \tag{3}$$

$$CC_g\frac{\partial T}{\partial t} = -\frac{1}{r^2}\frac{\partial}{\partial r}(r^2e) + (-\Delta H_3)\mathcal{R}_3 \tag{4}$$

where ν_i denotes the stoichiometric coefficient of the i^{th} species in the CO oxidation reaction. The radiant interaction between the particle surface and the environment is described by the single particle radiation model (Mon and Amundson, 1978). The boundary conditions at the particle surface, $r = a(t)$ are given by (Mon and Amundson, 1980),

$$N_1 = -\mathcal{R}_1; \; N_2 = -\mathcal{R}_2; \; N_3 = 2(\mathcal{R}_1 + \mathcal{R}_2) \tag{5}$$

$$\frac{a\rho_sC_s}{3m_c}\frac{dT_s}{dt} = \lambda\left(\frac{dT}{dr}\right)_{r=a(t)} - \sigma\epsilon(T_s^4 - T_B^4) + \sum_{i=1}^{2}\mathcal{R}_i(-\Delta H_i) \tag{6}$$

while at $r = b(t)$,

$$C_i = C_{iB}, \; i = 1 \text{ to } 3; \; T = T_B \tag{7}$$

Finally, the rate of change of particle size is given by:

$$\frac{da}{dt} = -\frac{m_c}{\rho_s}(2\mathcal{R}_1 + \mathcal{R}_2) \tag{8}$$

It is assumed that, as the particle size changes during combustion, the boundary layer thickness changes in such a way that the ratio $[b(t)/a(t)]$ remains constant. It has been shown by Sundaresan (1980) that the qualitative features of the steady state structure (and presumably the dynamics) are hardly sensitive to this assumption. The dimensionless variables and their definitions are given in Table 2. In terms of these variables, Eqs. 3 to 8 reduce to:

$$\delta_1\frac{\partial\theta}{\partial\tau} = \frac{1}{\psi^2s^4}\frac{\partial^2\theta}{\partial\xi^2} + \beta_3R_3 \tag{9}$$

TABLE 2. DEFINITIONS OF DIMENSIONLESS VARIABLES.

Variable	Definition	Variable	Definition
s	r/a	α	$1 - a/b$
ξ	$(1 - a/r)/\alpha$	θ	T/T^*
θ_i	$T_i/T^*, \; i = B, s$	R_i	$\frac{a^*\alpha\mathcal{R}_i}{CD}, \; i = 1, 2$
R_3	$\frac{a^{*2}\alpha^2\mathcal{R}_3}{CD}$	R_s	$2R_1 + R_2$
β_i	$\frac{(-\Delta H_i)CD}{\lambda T^*}$	Q	$\frac{\sigma\epsilon a^*\alpha T^{*3}}{\lambda}$
ψ	a/a^*	μ	$\frac{CDC_s}{3\lambda}$
δ_1	$\frac{\alpha m_c}{\rho_s} \cdot \frac{CDCC_g}{\lambda}$	δ_2	$\frac{Cm_c\alpha}{\rho_s}$
τ	$\frac{m_cCDt}{\rho_s\alpha a^{*2}}$		

$$\delta_2\frac{\partial y_i}{\partial\tau} = \frac{\gamma_i}{\psi^2s^4}\frac{\partial^2y_i}{\partial\xi^2} + \nu_iR_3, \; i = 1 \text{ to } 3 \tag{10}$$

for $0 < \xi < 1$. At $\xi = 0$

$$\gamma_1\frac{dy_1}{d\xi} = \psi R_1 \tag{11}$$

$$\gamma_2\frac{dy_2}{d\xi} = \psi R_2 \tag{12}$$

$$\gamma_3\frac{dy_3}{d\xi} = -2\psi(R_1 + R_2) \tag{13}$$

$$\mu\psi^2\frac{d\theta_s}{d\tau} = \left(\frac{\partial\theta}{\partial\xi}\right)_{\xi=0} + \psi\sum_{i=1}^{2}\beta_iR_i - \psi Q(\theta_s^4 - \theta_B^4) \tag{14}$$

while at $\xi = 1$

$$y_i = y_{iB}, \; i = 1 \text{ to } 3; \; \theta = \theta_B \tag{15}$$

The rate of change of particle size is given by:

$$\frac{d\psi}{d\tau} = -R_s \tag{16}$$

Let us denote the problem described by Eqs. 9 to 16 as the complete transient analysis. The constants δ_1 and δ_2 appearing in Eqs. 9 and 10 are usually very small indicating that the processes occurring inside the boundary layer are fast compared to the time constant associated with the rate of change of particle size. Thus it is reasonable to expect a quasisteady state assumption for the boundary layer processes to be adequate for practical purposes. Then, Eqs. 9 and 10 become:

$$\frac{1}{\psi^2s^4}\frac{d^2\theta}{d\xi^2} + \beta_3R_3 = 0 \tag{17}$$

$$\frac{\gamma_i}{\psi^2s^4}\frac{d^2y_i}{d\xi^2} + \nu_iR_3 = 0, \; i = 1 \text{ to } 3 \tag{18}$$

for $0 < \xi < 1$ and Eqs. 11 to 16 remain unchanged. By simplifying Eqs. 11 to 18 we obtain the following:

$$2\gamma_1y_1 + \gamma_2y_2 = \psi R_s(\xi - 1) + 2\gamma_1y_{1B} + \gamma_2y_{2B} \tag{19}$$

$$\gamma_2y_2 + \gamma_3y_3 = \psi R_s(1 - \xi) + \gamma_2y_{2B} + \gamma_3y_{3B} \tag{20}$$

$$\beta_3\gamma_2y_2 - \theta = \left[\beta_3R_2\psi - \left(\frac{d\theta}{d\xi}\right)_{\xi=0}\right](\xi - 1) + \beta_3\gamma_2y_{2B} - \theta_B \tag{21}$$

The quasisteady state analysis is now described by Eqs. 14-17 and 19 to 21. Mon and Amundson (1980) have employed the quasisteady state analysis to study the dynamics of carbon combustion.

Initial Conditions. For the quasisteady state analysis we must specify the initial particle size a_o and the initial particle temperature T_{so}. Usually for a given set of initial conditions ($\psi_o = a_o/a^*$; $\theta_{so} = T_{so}/T^*$), there is a unique set of temperature and concentration profiles in the boundary layer, i.e., Eqs. 11-13, 15, 17, 18 along with $\psi = \psi_o$ and $\theta(0) = \theta_s = \theta_{so}$ have a unique solution. Mon and Amundson (1980) have reported the possibility of multiplicity for this problem and if multiple solutions are possible, we must also specify the appropriate branch we are interested in. Conditions under which multiple solutions are possible are not explored in this publication. For the complete transient analysis, we must specify the initial concentration and temperature profiles in the boundary layer that are consistent with Eqs. 11-13, 15 along with the initial particle size.

Method of Solution

A variety of discretization procedures for converting the distributed system in a system of nonlinear ODE's are available, e.g. finite difference approximation, global collocation, spline collocation, etc. When there is significant CO oxidation in the boundary layer, the concentration and temperature profiles are usually very stiff; and a spline procedure turns out to be superior to global schemes. The interval $0 \leq \xi \leq 1$ is divided into a number of subintervals and in each subinterval the function is approximated by a cubic polynomial. We also impose the condition that at every node point the function as well as its first derivative must be continuous. The adjustable variable, chosen in order to obtain satisfactory representation of the given function, is the number of subintervals. The representation of the function can be greatly simplified by formalising the concept outlined above (Prenter, 1975). A representation of this kind is popularly known as Hermite polynomial approximation. The set of nonlinear ODE's obtained through discretization is integrated using the STIFF 3 routine discussed by Villadsen and Michelsen (1978). Since the boundary conditions at $\xi = 0$ (Eqs. 11-13) are nonlinear, Villadsen and Michelsen (1978) recommend that Eqs. 11 to 13 be replaced by:

$$\delta_3 \frac{\partial y_i}{\partial \tau} = \gamma_1 \frac{\partial y_i}{\partial \xi} - \psi R_1 \tag{11a}$$

$$\delta_3 \frac{\partial y_2}{\partial \tau} = \gamma_2 \frac{\partial y_2}{\partial \xi} - \psi R_2 \tag{12a}$$

$$\delta_3 \frac{\partial y_3}{\partial \tau} = \gamma_3 \frac{\partial y_3}{\partial \xi} + 2\psi(R_1 + R_2) \tag{13a}$$

at $\xi = 0$ and where δ_3 is a sufficiently small number. Extensive computations indicate that $\delta_3 \cong \delta_2/10$ is sufficient for good accuracy. Therefore, in the complete transient analysis we used Eqs. 11a-13a instead of Eqs. 11-13, with $\delta_3 = \delta_2/10$. We found that a Hermite polynomial approximation with six subintervals is adequate; this translates to a set of 53 nonlinear ODE's (initial value problem) in the case of a complete transient analysis and to a set of two nonlinear ODE's coupled with 51 algebraic equations in the case of quasisteady state analysis. Of these 51 algebraic equations, 39 are linear and 12 are nonlinear. This suggested a purely hypothetical model (discussed below) denoted by the pseudotransient analysis; where it is postulated that the carbon combustion is described by Eqs. 9, 14-16, 19-21. Thus, the only difference between the quasisteady state analysis and the pseudo transient analysis is that Eq. 17 is replaced by Eq. 9. The discretization procedure yields a set of 14 nonlinear ODE's coupled with 39 linear algebraic equations, in the case of pseudo transient analysis. All the three analyses yielded virtually indistinguishable results; however the pseudotransient analysis was relatively easier to program as well as least demanding in terms of computation time.

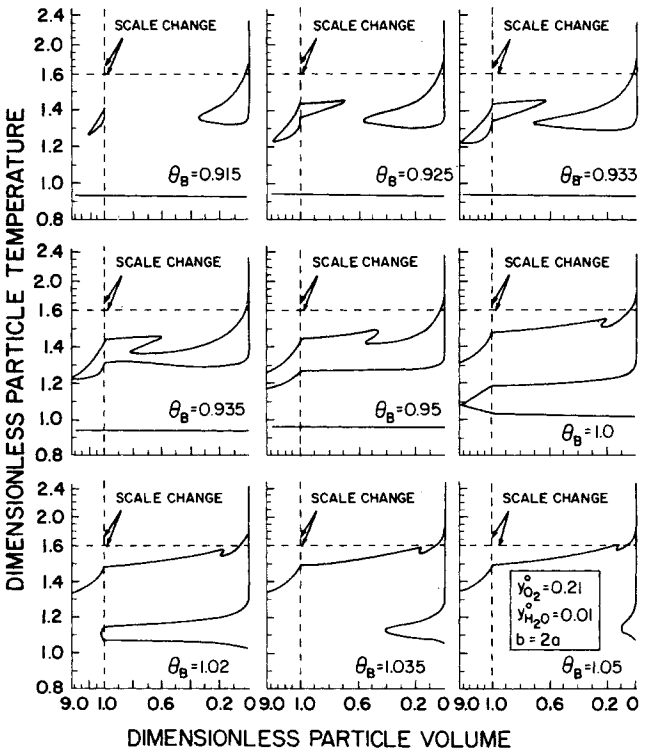

Figure 1. Steady-state structure: dimensionless particle temperature vs. dimensionless particle volume. Loci at different ambient temperatures. The ambient composition is the same for every figure. Broken lines and arrows indicate a change of scale.

RESULTS

The pseudosteady state problem underlying each of the three transient analyses mentioned earlier is the same. Figure 1 shows the genesis of the steady state structure for an ambient gas phase composition of 21% O_2, 1% H_2O and 78% N_2. In this figure the θ_s vs. dimensionless particle volume $(a/a^*)^3$ loci predicted by the pseudosteady state analyses at different ambient temperatures are shown. Sundaresan and Amundson (1980a) discuss in detail the structure shown in this figure. The pseudosteady state analysis predicts a unique unignited solution for a particle of dimensionless volume 0.9 at an ambient temperature of 915°K. Now, even if the initial temperature of this particle is very high, the particle will cool down rapidly and burn along the unignited branch.

For a somewhat higher ambient temperature ($\theta_B = 0.925$), the same particle now has three steady states. Hence, the particle, if its initial temperature is very high, will cool down until the ignited branch of the first lobe is reached and continue to burn along it. However, when the particle size has become small enough that the first lobe ceases to exist, it will 'see' only the unignited branch and therefore it will cool down rapidly and burn along the unignited branch thereafter. This may be classified as the thermal instability observed in other gas-solid reaction systems (Cannon and Denbigh, 1957; Shen and Smith, 1965; Beveridge and Goldie, 1968).

At higher ambient temperatures (say, $\theta_B = 0.933$), when the first lobe ceases to exist, the particle will catch the ignited branch of the second lobe and continue to burn along it. Thus, above some critical ambient temperature, the hot particle will sustain ignition. This is shown in Figure 2 where the particle temperature vs. particle radius histories for a particle of initial radius 1000μ corresponding to different furnace (ambient) temperatures are plotted. It is assumed that the particle is heated to 1500 K in an inert environment before being admitted into the

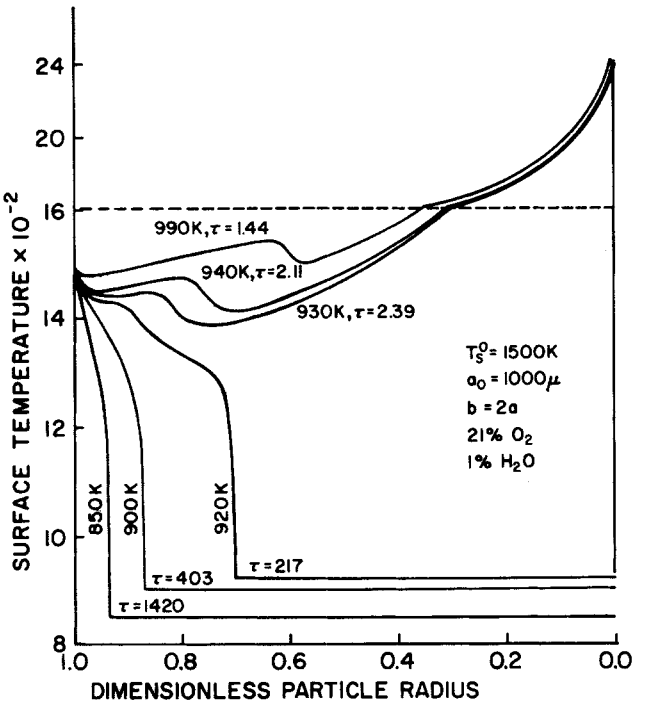

Figure 2. Particle temperature vs. dimensionless particle radius histories at different furnace (ambient) temperatures. The initial size and temperature of the particle, and the ambient composition are the same for every curve. τ denotes the dimensionless burnoff time.

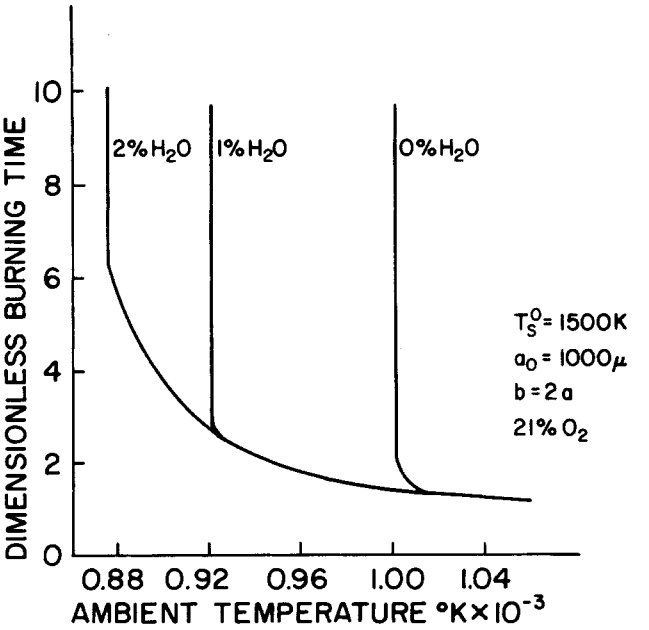

Figure 3. Dimensionless burnoff time at different furnace temperatures, for the particle whose initial size and temperature are given in Figure 2. The results corresponding to different water vapor levels in the gas phase are compared, while O_2 mole fraction is held constant at 0.21 on a wet basis.

furnace. As mentioned above, at low ambient temperatures the particle quenches rapidly and at somewhat higher furnace temperatures (920°K) the particle burns along the ignited branch of the first lobe until it ceases to exist at which time the particle is quenched.

Finally, at sufficiently high furnace temperatures the particle sustains ignition. The dimensionless burnoff times corresponding to different ambient temperatures are shown in Figure 2. [To obtain the burning time in seconds multiply the dimensionless burning time by 44.1.] Notice that there is a substantial reduction in the burning time when the particle sustains ignition. This is also shown in Figure 3 where we have plotted the burning time for the particle considered in Figure 2, at different furnace temperatures. We have compared the results corresponding to different water vapor levels in the gas phase while maintaining the O_2 fraction constant on a wet basis. The vertical lines indicate the critical ambient temperature above which the particle sustains ignition.

It is clear that as we increase the water vapor level the critical furnace temperature required for sustained ignition decreases. Notice that for sufficiently high ambient temperatures, the burning time is virtually independent of the water vapor level. However, the product composition is significantly different for different water vapor levels, as shown in Figure 4 where the fraction of carbon oxides leaving the boundary layer as CO_2 is plotted at different consumption levels. It is easy to see that the results corresponding to different water vapor levels are quite different. Focusing our attention on the 1% H_2O case at T_B = 990°K, we see that the product is predominantly CO_2 initially; however when the consumption is about 75% (by volume) there is a steep decrease in the CO_2 fraction. It can be seen in Figure 2 that this is accompanied by a decrease in the particle temperature. This happens when five steady states no longer exist (Figure 1), at which time the heterogeneous reactions sustain ignition while the homogeneous CO oxidation undergoes a (partial) quenching.

When the CO flame is extinguished, the net heat released in the vicinity of the particle decreases resulting in a decrease in the particle temperature. Now we can conclude from Figure 4 that increasing the water vapor level in the gas phase usually increases the fraction of carbon oxides leaving as CO_2, and more importantly it delays the quenching of the CO flame. Returning to Figure 2, notice that even when there is sustained ignition, quenching is observed when the particle size becomes vanishingly small. This happens when the particle size becomes so small that multiple steady states are no longer possible. This thermal instability for extremely small particles is inevitable.

Thus far, we have considered a particle which is initially very hot. It is equally important to examine the dynamics of a particle that is initially cold. Here we define a cold particle as one whose initial temperature is lower than the furnace temperature. Let us return to Figure 1 and consider a particle of initial radius 1000μ, i.e., $[a/a^*]^3 = 1.0$. If $\theta_B = 0.915$, the cold particle will see the unignited steady state as the nearest (or the only) attractor. Hence the particle temperature will rise rapidly until the value corresponding to the lowest steady state is attained and thereafter the burning will follow the unignited branch. In other words, this particle will not be ignited at an ambient temperature of 915°K.

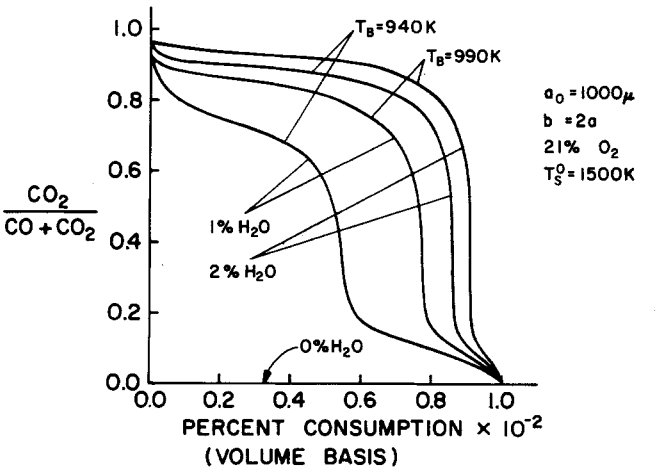

Figure 4. The fraction of carbon oxides leaving the external edge of the boundary layer as CO_2 (for the particle whose initial size and temperature are given in Figure 2) is plotted against percent consumption. The histories for different furnace temperatures and water vapor levels are compared.

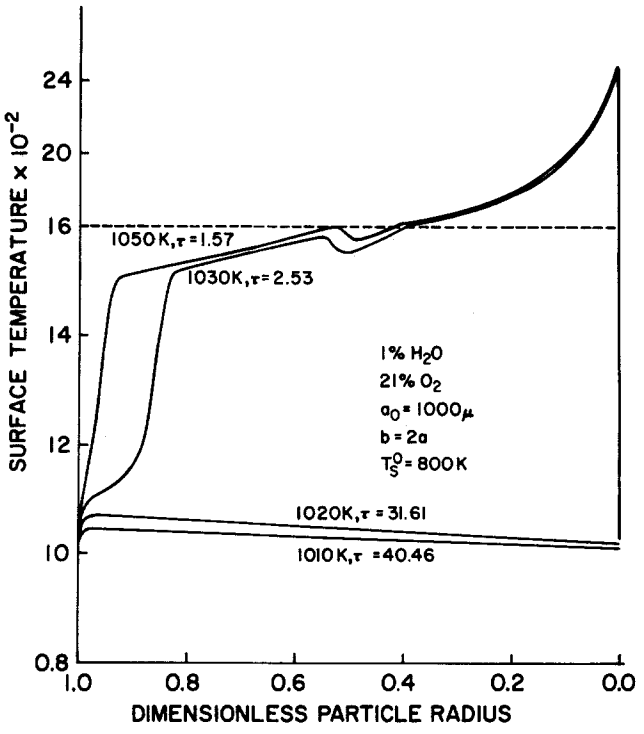

Figure 5. Same as Figure 2.

Following the same argument this particle will not be ignited even if the ambient temperature is 1020°K. However, when $\theta_B = 1.035$, this particle will see the ignited branch as the only attractor and therefore the particle will ignite. Thus we may expect that there exists a critical ambient temperature above which a cold particle will become ignited. This is shown in Figure 5 which presents the particle temperature vs. particle radius histories for a particle of radius 1000μ at different furnace temperatures. The initial temperature of the particle is 800°K. As mentioned above, the particle does not ignite for low ambient temperatures while at sufficiently high ambient temperatures the particle ignites.

The thermal instability for extremely small particles discussed along with Figure 2 is seen in Figure 5 as well; and is inevitable. This has been observed experimentally by Ubhayakar and Williams (1976) and Ubhayakar (1976) has advanced a theoretical model for this instability. Notice in Figure 5 that there is a

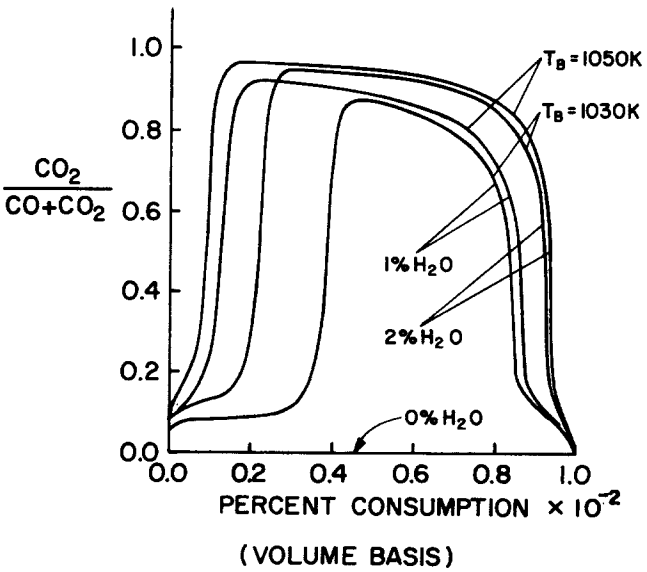

Figure 7. Same as Figure 4.

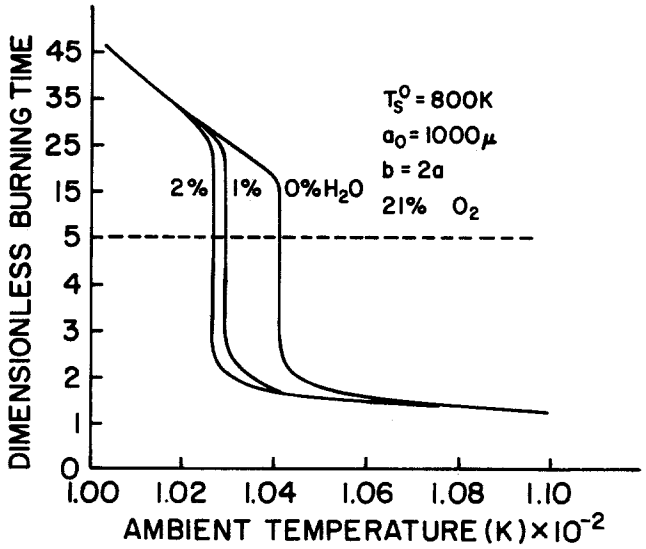

Figure 6. Same as Figure 3.

substantial reduction in the burning time when the particle ignites. This is also seen in Figure 6 where we have plotted the burning time for the particle considered in Figure 5 at different furnace temperatures. We have compared the results corresponding to different water vapor levels while maintaining the O_2 fraction constant on a wet basis. The vertical lines indicate the critical ambient temperature above which the particle will be ignited. When we increase the water vapor level this critical temperature decreases slightly.

For sufficiently high ambient temperatures, the burning time is virtually independent of water vapor level. However, as discussed in the context of a hot particle, the product composition is quite different for different water vapor levels, as shown in Figure 7. Initially, as the particle temperature is low, there is very little CO oxidation in the boundary layer. As the particle heats up, the extent of CO oxidation increases rapidly approaching the pseudosteady state value. The sudden drop in the fraction of carbon oxides leaving as CO_2 at large consumption levels is due to a (partial) quenching of the CO flame in the boundary layer which is accompanied by a decrease in the particle temperature (Figure 5). It is now clear that the contribution of water

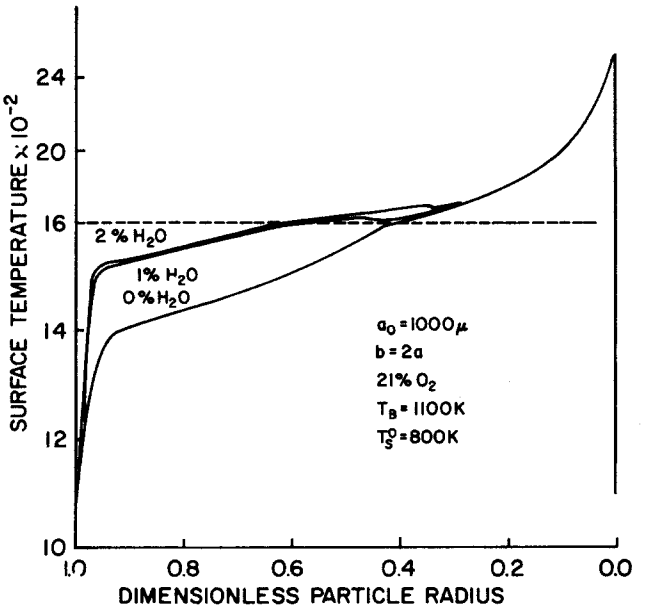

Figure 8. Particle temperature vs. dimensionless particle radius histories at different water vapor levels in the gas phase. The mole fraction of O_2 is held constant on a wet basis.

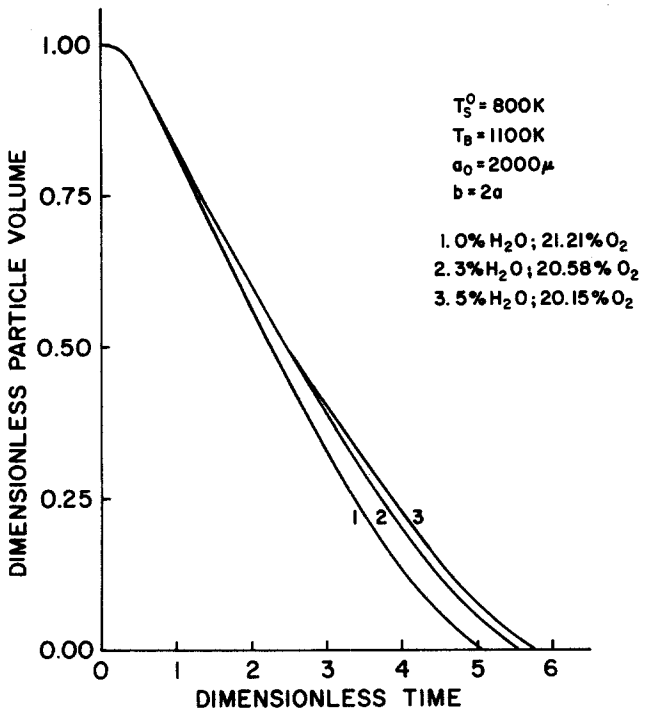

Figure 9. Dimensionless particle volume vs. dimensionless time histories at different water vapor levels in the gas phase. The mole fraction of O_2 is held constant on a dry basis.

vapor towards combustion of a particle that is initially cold is very similar to that of a particle which is initially hot.

In the experiments of Smith and Gudmundsen (1931), the particle is first heated to the furnace temperature by inert gas and then the gaseous reactants are admitted into the furnace. The carbon particles become ignited in both dry and humid air. Hence, for a proper comparison of the model with experiments, we must consider the case where the particle is initially cold with respect to the furnace temperature and the furnace temperature must be sufficiently large (Figure 6) that there is ignition at all water vapor levels. Figure 8 shows a comparison of the particle temperature histories under different water vapor levels in the gas phase while the O_2 fraction is held constant on a wet basis. The particle does indeed burn at a higher temperature in moist air compared to dry air conditions. This is clearly due to the exothermic CO oxidation in the boundary layer.

However at some point the CO flame in the boundary layer is quenched at which time the temperature of the particle burning in moist air decreases and reaches the value corresponding to dry air conditions. Thus the model is in qualitative agreement with the observations of Smith and Gudmundsen (1931) that: (i) carbon particles burn at a higher temperature in moist air compared to dry air conditions; and (ii) this temperature difference vanishes as the particle size becomes sufficiently small. However, the model predicts that the burning time (corresponding to Figure 8) is virtually independent of the water vapor level. This is definitely not in agreement with the experiments of Smith and Gudmundsen (1931).

For a proper comparison between theory and experiments, we should have held the O_2 level in the gas phase constant on a dry basis. We chose the case where the O_2 level is held constant on a wet basis in order to isolate the catalytic effect of water vapor and study it separately. Sundaresan (1980) has reported the results when the O_2 level is held constant on a dry basis. Briefly, none of the results presented so far change noticeably. However, the burning time is no longer independent of water vapor level, as shown in Figure 9 for a somewhat larger particle. The particle does indeed burn at a slower rate in moist air. However, it must be conceded that: (i) the difference in the combustion rates in dry and moist air conditions predicted by the model is much smaller than the experimentally observed value; and (ii) this difference would probably vanish if the reaction between carbon and water vapor is included.

We conclude that to explain the experimental results on burning rate, a more sophisticated kinetic model accounting for competition between O_2, H_2O and CO_2 for active sites at the carbon surface must be considered. Consequently, we did not attempt any quantitative comparison between the model and the experiments. Nevertheless, a little reflection should reveal that the pathology reported in this study stems from the interac-

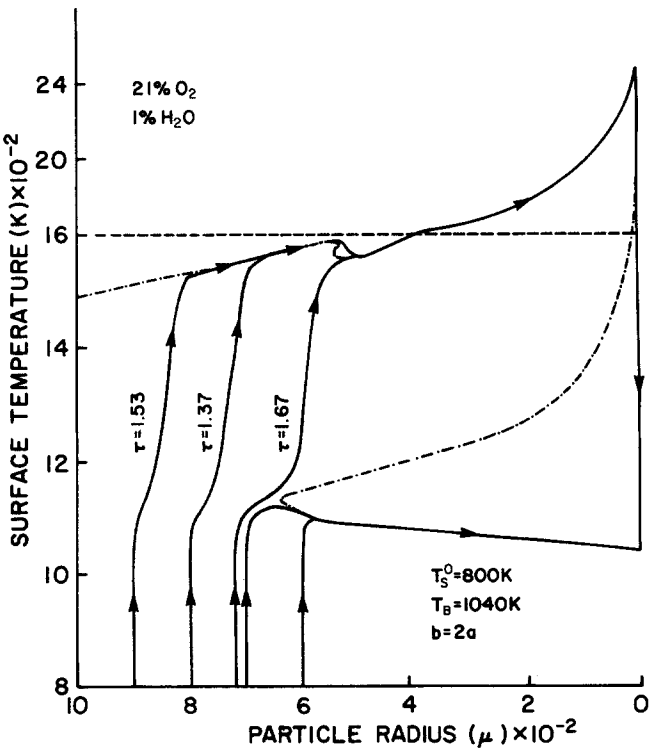

Figure 10. Particle temperature vs. particle radius histories for particles of different initial sizes. Solid lines indicate the combustion trajectories; - - - denotes a change of scale; — · — · — denotes the pseudosteady-state locus.

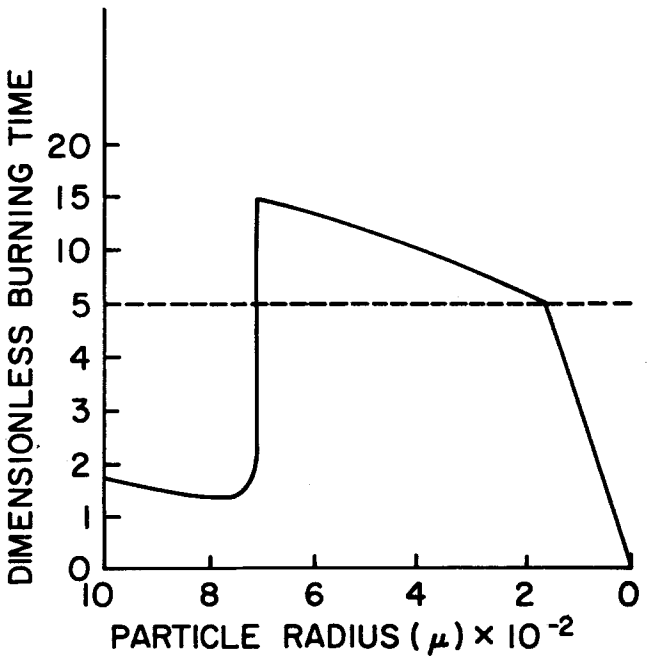

Figure 11. Dimensionless burnoff times for particles of different initial sizes. The furnace conditions are as given in Figure 10.

tion between transport and reaction in the boundary layer. Therefore, a more sophisticated kinetic model is unlikely to destroy the structure reported here.

This study revealed another interesting feature, presented in Figure 10. The broken line indicates the pseudosteady state trajectory for the set of ambient conditions reported there. A particle of radius 900μ sees the ignited branch as the only attractor and therefore ignition results. However a smaller particle (radius 600μ) sees the unignited branch as the nearest attractor and hence fails to ignite. Thus a large particle ignites while a small particle fails to do so. The burning times for different initial particle sizes are given in Figure 11. It is clear that the lack of ignition for a small particle has results in a substantial increase in the burning time and we have a situation where a larger particle requires a shorter time to burn off completely (compare the burnoff times for 600μ and 900μ particles). This indicates that the popular belief that crushing the carbon particle will result in a more efficient combustion is suspect.

CONCLUSION

The dynamics of a single-particle carbon combustion is analysed when the O_2 level in the gas phase is large. The effects of water vapor on the combustion characteristics are discussed. The model agrees qualitatively with part of the experimental data of Smith and Gudmundsen (1931). To obtain a better agreement with the experimental data, a more sophisticated kinetic model accounting for competition between O_2, H_2O and CO_2 for active sites at the carbon surface is probably needed. If the O_2 level is substantially smaller than the value used in this study, pseudosteady state structures less complex than Figure 1 are obtained (Sundaresan and Amundson, 1980a). The dynamic features of these subcases can be deduced rather easily from the analysis presented in this paper.

ACKNOWLEDGMENT

This work was supported by a grant from the Department of Energy.

NOMENCLATURE

a = radius of the particle
a_o = initial radius of the particle
a^* = radius of a reference particle = 1000μ
b = radius of the outer edge of the boundary layer
c = total concentration
c_i = concentration of i^{th} species
C_g, C_s = heat capacity of gas and solid respectively
D = diffusivity defined in Eq. 1
D_{ij} = binary diffusion coefficient
e = flux of sensible energy
E_i = activation energy of i^{th} reaction
(ΔH_i) = heat of i^{th} reaction
k_i = pre-exponential factor for i^{th} reaction
m_c = molecular weight of carbon
N_i = flux of species i
Q = see Table 2
r = radial coordinate
$\mathcal{R}_i$ = rate of i^{th} reaction
R_i = dimensionless rate of i^{th} reaction (Table 2)
s = dimensionless radial coordinate
t = time variable
T = temperature
T^* = reference temperature = 1000°K
y_i = mole fraction of i^{th} species

Subscripts

s, B = denote values of a variable at the particle surface and in the ambient gas phase respectively
o = initial value of a variable

Greek Letters

α, β_i, ξ, ψ, μ, δ_i, θ, τ = see Table 2
γ_i = multicomponent diffusivity ratio
ν_i = stoichiometric coefficient of species i, in the CO oxidation reaction
λ = thermal conductivity of the gas
ρ_s = density of the solid
ϵ = emissivity of the surface
σ = Stefan-Boltzmann constant

LITERATURE CITED

Beveridge, G. S. G., and P. J. Goldie, "Effectiveness factors and instability in non-catalytic gas-solid reactions: the effect of solid heat capacity," *Chem. Eng. Sci.*, **23**, 913 (1968).

Cannon, K. J., and K. G. Denbigh, "Studies on gas solid reactions I and II," *Chem. Eng. Sci.*, **6**, 145, 155 (1957).

Caram, H. S., and N. R. Amundson, "Diffusion and Reaction in a Stagnant Boundary Layer about a Carbon Particle," *Ind. Eng. Chem. Fund.*, **16**, 171 (1977).

Dutta, S., C. Y. Wen and J. Belt, "Reactivity of Coal and Char in a CO_2 Atmosphere," Prepr., Div. Fuel Chem., Am. Chem. Soc., **20**(3), 103 (1975).

Field, M. A., D. W. Gill, B. B. Morgan, and P. G. W. Hawksley, "Combustion of Pulverized Coal," BCURA Leatherhead, Cherey and Sons, Ltd., Banbury, England (1967).

Howard, J. B., G. C. Williams, and D. H. Fine, "Fourteenth Symposium (International) on Combustion," The Combustion Institute, Pittsburgh, PA 975 (1973).

Mon, E., and N. R. Amundson, "Diffusion and Reaction in a Stagnant Boundary Layer about a Carbon Particle. II. An Extension," *Ind. Eng. Chem. Fund.*, **17**, 313 (1978).

Mon, E., and N. R. Amundson, "Diffusion and Reaction in a Stagnant Boundary Layer about a Carbon Particle. IV. The Dynamical Behavior," *Ind. Eng. Chem. Fund.*, (Submitted in 1980).

Prenter, P. M., *Splines and Variational Methods*, Ch. 3, Wiley-Interscience, John Wiley and Sons (1975).

Shen, J., and J. M. Smith, "Diffusional Effects in Gas-Solid Reactions," *Ind. Eng. Chem. Fund.*, **4**, 293 (1965).

Smith, D. F., and A. Gudmundsen, "Mechanism of Combustion of Individual Particles of Solid Fuels," *Ind. Eng. Chem.*, 277 (1931).

Sundaresan, S., "Model Studies on Carbon Combustion," Ph.D. dissertation, University of Houston (1980).

Sundaresan, S., and N. R. Amundson, "Diffusion and Reaction in a Stagnant Boundary Layer about a Carbon Particle. V. Pseudo Steady State Structure and Parameter Sensitivity," *Ind. Eng. Chem. Fund.* (Submitted in 1980).

Sundaresan, S., and N. R. Amundson, "Diffusion and Reaction in a Stagnant Boundary Layer about a Carbon Particle. VI. Effect of Water Vapor on Pseudo Steady State Structure," *Ind. Eng. Chem. Fund.* (Submitted in 1980).

Ubhayakar, S. K., and F. A. Williams, "Burning and Extinction of a Laser-ignited Carbon Particle in Quiesant Mixtures of Oxygen and Nitrogen," *J. Electrochem. Soc.*, **123**, 5, 747 (1976).

Ubhayakar, S. K., "Burning Characteristics of a Spherical Particle Reacting with Ambient Oxidizing Gas at its Surface," *Combustion and Flame*, **26**, 23 (1976).

Villadsen, John and M. L. Michelsen, *Solution of Differential Equation Models by Polynomial Approximation*, 322, 341 Problem No. 13, Prentice-Hall, Inc., Englewood Cliffs, NJ (1978).

Manuscript received June 18, 1980; revision received October 7, and accepted October 20, 1980.